5′-Deoxyadenosine Contacts the Substrate Radical Intermediate in the Active Site of Ethanolamine Ammonia-lyase: ^{2}H and ^{13}C Electron Nuclear Double Resonance Studies†

Russell LoBrutto,‡ Vahe Bandarian,§,|| Olafur Th. Magnusson,§ Xiangyang Chen,⊥,# Vern L. Schramm,⊥ and George H. Reed*,§

Department of Plant Biology, Arizona State University, Tempe, Arizona 85287-1601, Department of Biochemistry, University of Wisconsin—Madison, Madison, Wisconsin 53705, and Department of Biochemistry, Albert Einstein College of Medicine, 1300 Morris Park Avenue, Bronx, New York 10461-1975

Received August 8, 2000

ABSTRACT: The mechanism of propagation of the radical center between the cofactor, substrate, and product in the adenosylcobalamin- (AdoCbl) dependent reaction of ethanolamine ammonia-lyase has been probed by pulsed electron nuclear double resonance (ENDOR) spectroscopy. The radical of *S*-2-aminopropanol, which appears in the steady state of the reaction, was used in ENDOR experiments to determine the nuclear spin transition frequencies of ^{2}H introduced from either deuterated substrate or deuterated coenzyme and of ^{13}C introduced into the ribosyl moiety of AdoCbl. A ^{2}H doublet (1.4 MHz splitting) was observed centered about the Larmor frequency of ^{2}H. Identical ENDOR frequencies were observed for ^{2}H irrespective of its mode of introduction into the complex. A ^{13}C doublet ENDOR signal was observed from samples prepared with [U-^{13}C-ribosyl]-AdoCbl. The ^{13}C coupling tensor obtained from the ENDOR powder pattern shows that the ^{13}C has scalar as well as dipole−dipole coupling to the unpaired electron located at C1 of *S*-2-aminopropanol. The dipole−dipole coupling is consistent with a distance of 3.4 ± 0.2 Å between C1 of the radical and C5′ of the labeled cofactor component. These results establish that the C5′ carbon of the 5′-deoxyadenosyl radical moves ∼7 Å from its position as part of AdoCbl to a position where it is in contact with C1 of the substrate which lies ∼12 Å from the Co^{2+} of cob(II)alamin. These findings are also consistent with the contention that 5′-deoxyadenosine is the sole mediator of hydrogen transfers in ethanolamine ammonia-lyase.

Transfers of hydrogen atoms between cofactor, substrates, and products are a hallmark of enzymes catalyzing AdoCbl[1]-dependent rearrangement reactions (*1*). Such transfers have been documented for EAL—a bacterial enzyme that catalyzes the deamination of vicinal amino alcohols—using tritium isotope tracer techniques (*2*). These transfers are illustrated in the attractive model of the catalytic cycle of EAL in Scheme 1. However, unusually large KIEs on the washout of tritium from labeled cofactor (*3*) and the fact that the substrate-derived radicals of EAL are positioned >10 Å from the low-spin Co^{2+} of cob(II)alamin (*4*) have called into question the simplicity of this elegant scheme. A more complicated scheme in which a group from the protein carries the radical center for the majority of catalytic cycles under conditions of V_{max} has been proposed (*5*). In the revised scheme, the AdoCbl does not reform at the end of each catalytic cycle. There is a report of a small pool of volatile ^{3}H in EAL whenever tritiated ethanolamine is being processed (*6*). This pool could be from the putative protein group. However, ^{3}H washes out from this pool at the same rate as ^{3}H from the cofactor, so the significance of the volatile pool, in the context of the putative protein radical, is not clear.

During the single turnover inactivation of EAL by deuterated hydroxyethylhydrazine, all of the 5′-deoxyadenosine contains at least one ^{2}H—a finding consistent with direct exchange of ^{2}H between the inactivator and the cofactor fragment without an intermediary group from the protein (*7*). Moreover, the pool size of exchangeable ^{2}H determined from stopped-flow kinetic experiments is consistent with the content of the 5′-methylene group of AdoCbl (*8*). These latter observations suggested that the 5′-deoxyadenosyl radical might shuttle several Ångstroms from its position near Co^{2+} following cobalt−carbon bond homolysis to become 5′-deoxyadenosine by abstraction of a hydrogen from the

† This work was supported by NIH Grants GM 35752 (G.H.R.) and GM41916 (V.L.S.) and NSF Grant BIR-9601774 (R.L.). O.Th.M. was supported by the Sam C. Smith predoctoral fellowship administered by the Department of Biochemistry, University of Wisconsin—Madison.

* To whom correspondence should be addressed.
‡ Arizona State University.
§ University of Wisconsin—Madison.
|| Present address: Biophysics Research Division, University of Michigan, Chemical Sciences Bldg., 930 N. University Ave., Ann Arbor, MI 48109-1055.
⊥ Albert Einstein College of Medicine.
Present address: Monsanto Company, 800 N. Lindberg Blvd., MZ Q3A, St. Louis, MO 63167.

[1] Abbreviations used: AdoCbl, adenosylcobalamin; CW, continuous wave; EAL, ethanolamine ammonia-lyase; EPR, electron paramagnetic resonance; ENDOR, electron nuclear double resonance; Hepes, *N*-2-hydroxyethylpiperazine-*N*′-2-ethanesulfonic acid; KIE, kinetic isotope effect; rf, radio frequency.

10.1021/bi001865s CCC: $20.00
Published on Web 12/12/2000

Scheme 1

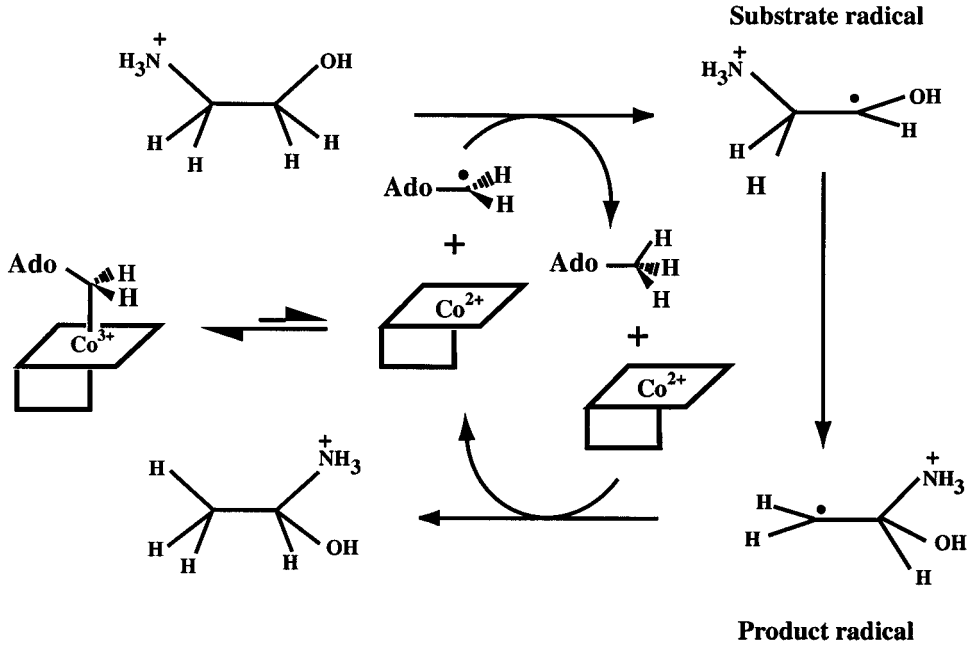

substrate. Following its regeneration by loss of a hydrogen atom to the product radical, the 5′-deoxyadenosyl radical moves back into position where it recombines with the cob(II)alamin at the end of the catalytic cycle. Magnetic field effects (*9*) on *V*/*K* are also indicative of a radical recombination event such as that given in Scheme 1. There is also a suggestion, from temperature dependence studies of the ^{2}H kinetic isotope effects (*3*), that the unusually large ^{3}H KIEs are an indication of tunneling in the hydrogen transfer steps. This paper reports the results of pulsed ENDOR spectroscopic measurements that place the 5′-methyl of 5′-deoxyadenosine in direct contact with the half-occupied *p* orbital of the substrate radical. This observation provides strong support for the viability of Scheme 1 for EAL and for the proposed shuttling function of the coenzyme fragment.

EXPERIMENTAL PROCEDURES

Materials. EAL from *Salmonella typhimurium* (plasmid pKQE4.5, generous gift from Dr. B. Babior, Scripps Research Institute, La Jolla, CA) was expressed in *Escherichia coli* and purified as described previously (*10*). The protein had a specific activity of 50 IU mg^{-1} in the coupled assay with alcohol dehydrogenase. [1,1-$^{2}H_2$]-*S*-2-Aminopropanol was synthesized from L-alanine methyl ester as described previously (*8*). [5′,5′-$^{2}H_2$]-AdoCbl was synthesized by the method described previously (*11*) with minor modifications (*8*).

Synthesis of [U-^{13}C-ribosyl]ATP. Enzymatic synthesis was used to convert [U-^{13}C-glucose] into [U-^{13}C-ribosyl]ATP in a single coupled reaction mixture (*12*−*14*). The mixture (5 mL) contained 10 μmol of [U-^{13}C-glucose] (99 atom % ^{13}C) (Martek Biosciences Corporation, Columbia, MD), 2 U of glucose-6-phosphate dehydrogenase, 2 U of 6-phosphogluconate dehydrogenase, 20 U of phosphoriboisomerase, 2 U of 5-phosphoribosyl-1-pyrophosphate synthetase, 1 U of adenine phosphoribosyltransferase, 20 U of myokinase, 40 U of pyruvate kinase, 10 U of glutamate dehydrogenase, 0.1 mM ATP, 10 mM $MgCl_2$, 20 mM PEP, 1 mM $NADP^+$, 3 mM adenine, 10 mM α-ketoglutarate, 50 mM potassium phosphate (pH 7.8), and 50 mM glycylglycine (pH 7.5). After being incubated for 5 min at 37 °C, 20 U of hexokinase was added to initiate the synthesis. Most enzymes were supplied as ammonium sulfate suspensions (Sigma, St. Louis) and were used without further treatment. Adenine phosphoribosyltransferase was isolated from *E. coli* K12 (*13*). Sufficient NH_4^+ is introduced with the enzymes to provide substrate for the glutamate dehydrogenase reaction. Reaction mixtures were incubated at 37 °C for an additional hour, and the reaction was terminated by heating to 95 °C for 1 min followed by centrifugation. Purification of the labeled ATP was on C18 reverse-phase HPLC, eluting with 50 mM triethylammonium acetate (pH 6.0) containing 5% methanol. Note that the final ATP product is a combination of the unlabeled ATP added to the reaction mixture and that produced by the synthetic reactions. On the basis of the yield from [U-^{13}C-glucose], the ratio of [U-^{13}C-glucose]ATP to natural abundance ATP is approximately 12:1. NMR analysis of ^{13}C and proton spectra confirmed the uniform incorporation of ^{13}C into the ribose ring but not the purine ring.

Synthesis of [1′,2′,3′,4′,5′-$^{13}C_5$]-AdoCbl. This step was performed enzymatically using the ATP:corrinoid adenosyltransferase (CobA) from *S. typhimurium* with [U-^{13}C-ribosyl]ATP and cob(I)alamin as substrates. An *E. coli* overproducing strain JE2875 from a pT7-7 plasmid in BL21(DE3) cells was a generous gift of Prof. J. C. Escalante-Semerena, University of Wisconsin—Madison. Cells were grown in LB media, induced by 0.5 mM IPTG, and harvested 6 h after induction. CobA was purified as described elsewhere (*15*). The purified enzyme was precipitated by ammonium sulfate and resuspended in anaerobic Tris-H_2SO_4 (50 mM, pH 8).

The enzymatic reaction was carried out under inert atmosphere in a Coy anaerobic chamber. All solutions were flushed with O_2-free argon gas before use. The reaction

mixture contained 10 mM Tris-H_2SO_4 (pH 8), 1.6 mM $MgCl_2$, and 4 μmol of hydroxocob(III)alamin in a total volume of 20 mL. Hydroxocob(III)alamin was converted to cob(I)alamin using 50 μmol of titanium(III) citrate as a reducing agent (*16*), and the enzymatic reaction was initiated by the addition of 3.4 μmol of [U-^{13}C-ribosyl]ATP and 5 mg of CobA. Progress of the reaction was monitored by HPLC using a semipreparative C18 column (Phenomenex, 250 $\times$ 10 mm) with a gradient of 20−100% MeOH containing 0.02% TFA in 25 min. Cob(III)alamin has a retention time of 11 min, and AdoCbl elutes after 19 min under these conditions. The protein was separated from the cobalamins after a 3-h incubation using an Amicon ultrafiltration apparatus with a YM10 membrane. The filtrate was concentrated by rotary evaporation, and [U-^{13}C-ribosyl]-AdoCbl was purified by the HPLC method described above. Fractions containing the product were adsorbed onto a C18 Sep-Pak column, residual TFA washed off with water, and [U-^{13}C-ribosyl]-AdoCbl eluted with MeOH. The eluate was evaporated to dryness, redissolved in water, and frozen for storage. The product was indistinguishable from an authentic sample of AdoCbl (Sigma) as judged by UV−Vis spectroscopy.

Sample Preparation. Samples contained 0.01 M Hepes (pH 7.4), 0.20−0.24 mM (active sites) EAL, 0.40−0.48 mM unlabeled or labeled AdoCbl, and 0.025 M *S*-2-propanolamine. Samples were frozen within 20 s of mixing EAL with AdoCbl and *S*-2-propanolamine. All solutions containing AdoCbl were protected from ambient light.

ENDOR Spectroscopy. Pulsed ENDOR spectra were obtained using a Bruker ELEXSYS E580 FT-EPR spectrometer system. A Bruker EN4118X-MD5 ENDOR probehead, featuring a dielectric resonator with an integrated radio frequency (rf) saddle coil, was used. The probe was housed in an Oxford Instruments liquid helium cryostat. When loaded with a frozen sample for measurement at 15−20 K, the resonant frequency of the probe was 9.7 GHz. All ENDOR spectra were obtained using the Mims (*17*) pulse sequence, consisting of three $\pi/2$ microwave pulses and a single rf pulse between the second and third microwave pulses. The pulse train repetition rate was 1 kHz. An ENI A-500 CW rf power amplifier, having its nominal 500 W output attenuated by 2−3 dB was used to produce the high-power rf pulses. An rf pusle width of 7−8 μs, a delay of 12 μs between microwave pulses 2 and 3, and a $\pi/2$ microwave pulse width of 64 ns were used.

ENDOR spectra were simulated using the program GENDOR, written by Dr. P. Doan of Northwestern University. Because the GENDOR is for general ENDOR simulations, effects that are specific to particular pulsed ENDOR methods (such as "dead spots" in Mims ENDOR) are not accounted for in the calculations.

For a nucleus with spin I, coupled to an unpaired electron ($S = 1/2$), there exist $2I$ nuclear spin transitions of the type $\Delta m_I = \pm 1$ in each of the two electronic submanifolds. For ^{13}C ($I = 1/2$), the transition frequencies are given by the approximate expression (*18*):

$$\nu_{\pm} = |\nu_N \pm A_N/2| \quad (1)$$

where ν_N is the nuclear Larmor frequency, and A_N is the nuclear hyperfine coupling constant. For the case of ^{2}H ($I = 1$), the transition frequencies are

$$\nu_{\pm} = |\pm A_N/2 + \nu_N \pm 3P/2| \quad (2)$$

where P is the nuclear quadrupole coupling constant. If P is too small to produce a resolved splitting (i.e., $P \approx 0$), then eq 2 reduces approximately to eq 1. For the specific case where $|A_N/2| < \nu_N$ (as in the present study, for both ^{2}H and ^{13}C), the two observed transition frequencies are separated by A_N and centered about ν_N.

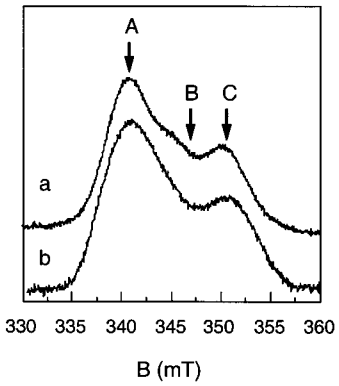

FIGURE 1: Spin−echo-detected EPR spectra of the trapped, substrate-based radical in EAL: (a) Substrate is [1,1-$^2H_2$]-*S*-2-aminopropanol, and AdoCbl has natural isotopic abundance. (b) Ribosyl moiety of AdoCbl is uniformly labeled with ^{13}C, and substrate has natural isotopic abundance. Points A (340.5 mT), B (346.5 mT), and C (350.5 mT) indicate three of the magnetic field settings where ENDOR measurements were performed. Experimental conditions: (a) microwave frequency (ν_e) = 9.695 GHz; T = 20 K; τ = 0.140 μs. (b) ν_e = 9.697 GHz; T = 15 K; τ = 0.210 μs. Pulse repetition rate = 1.00 kHz. Each data point is sum of 40 (a) or 100 (b) individual two-pulse echoes. Curves are displayed on different vertical scales.

RESULTS

The electron spin−echo (ESE)-detected EPR absorption of the radical in the steady state of the reaction with [1,1-$^2H_2$]-*S*-2-aminopropanol is shown in Figure 1a. The *y*-axis represents the integrated amplitude of the two-pulse spin−echo; therefore, the spectrum resembles a directly detected CW EPR absorption spectrum. The arrows indicate the magnetic field settings from which the ENDOR spectra in Figure 2 were obtained. The EPR absorption from the radical extends over ~200 G. The broad absorption is due primarily to a weak exchange and to a dipole−dipole interaction between the radical and the low spin Co^{2+} of cob(II)alamin with which the radical shares the active site. The absorption envelope also contains unresolved nuclear hyperfine splitting. The microwave pulses excite EPR transitions over a range of only about 10−15 G. Subpopulations of the radical, which are responsible for EPR absorption at various points in the spectrum, correspond to different directions of the magnetic field in a molecule-fixed axis system. Thus, ENDOR spectra obtained at different positions across the EPR absorption are sampling different orientations of the complex with respect to the laboratory field.

The ESE-detected EPR absorption spectrum of the intermediate radical formed in the steady state of the reaction with *S*-2-aminopropanol and [U-^{13}C-ribosyl]-AdoCbl is shown in Figure 1b. The presence in this sample of ^{1}H instead

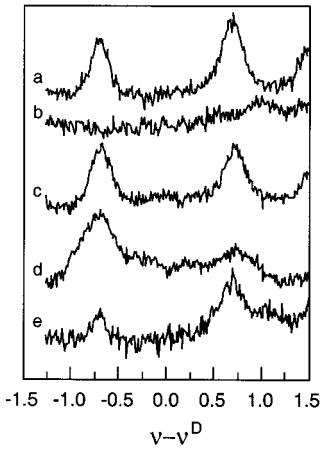

FIGURE 2: Mims ENDOR of trapped substrate radical in EAL. (a) Substrate is [1,1-$^2H_2$]-*S*-2-aminopropanol; $B_0 = 340.5$ mT; $\tau = 0.120$ μs; $t_{rf} = 8$ μs; $\nu_e = 9.700$ GHz. Each point is the sum of 4800 echoes. (b) Substrate and AdoCbl have natural isotopic abundance; $B_0 = 340.5$ mT; $\tau = 0.120$ μs; $t_{rf} = 8$ μs; $\nu_e = 9.700$ GHz; each point is the sum of 4800 echoes. (c) Substrate is [1,1-$^2H_2$]-*S*-2-aminopropanol; $B_0 = 350.5$ mT; $\tau = 0.160$ μs; $t_{rf} = 8$ μs; $\nu_e = 9.695$ GHz. Each point is the sum of 5400 echoes. (d) Substrate is [1,1-$^2H_2$]-*S*-2-aminopropanol; $B_0 = 346.5$ mT; $\tau = 0.160$ μs; $t_{rf} = 8$ μs; $\nu_e = 9.695$ GHz. Each point is the sum of 5400 echoes. (e) Substrate has natural isotopic abundance, and cofactor is [5′,5′-$^2H_2$-ribosyl]-AdoCbl; $B_0 = 340.5$ mT; $\tau = 0.120$ μs; $t_{rf} = 8$ μs; $\nu_e = 9.700$ GHz. Each point is sum of 28 800 echoes. Pulse sequence repetition rate = 1.0 kHz, and temperature = 15−20 K in all cases.

of ^2H at C1 of the substrate produces a somewhat broader absorption spectrum than that shown in Figure 1a.

^2H ENDOR. The Mims ENDOR spectrum obtained from the low-field absorption peak (point A) of the sample prepared with [1,1-$^2H_2$]-*S*-2-aminopropanol is shown in Figure 2a. The spectrum exhibits a doublet signal centered about the Larmor frequency of ^2H (2.26 MHz) that is not present under the same conditions in a matched sample prepared with unlabeled substrate (Figure 2b). The 1.4 MHz splitting of this signal is too small to be assigned to the ^2H remaining at the C1 of the [1,1-$^2H_2$]-*S*-2-aminopropanol, which has a much stronger interaction with the unpaired electron.[2] The ^2H ENDOR spectrum obtained from the high-field peak C of the EPR absorption (Figure 2c) also exhibits a sharp doublet having an identical splitting to that shown in Figure 2a. At intermediate magnetic field positions such as peak B (346.5 mT, Figure 2d), the ^2H doublet peaks are much broader, and the spectra have line shapes more indicative of powder patterns.

The intensity and persistence of the ^2H ENDOR doublet signal suggest that these peaks arise from the statistically favored orientation in which the magnetic field is perpendicular to the electron−nuclear interspin vector. Because the corresponding "parallel" features are not readily apparent and there is a strong possibility for a scalar coupling, direct extraction of the principal values of the hyperfine coupling tensor is not possible. However, consideration of the combined ^{13}C and ^2H ENDOR data sets leads to a meaningful estimate of the ^2H to radical distance (vide infra).

The ^2H ENDOR frequencies obtained when EAL is combined with [5′,5′-$^2H_2$]-AdoCbl and with protiated substrate are virtually identical to those obtained from the sample made up from [1,1-$^2H_2$]-*S*-2-aminopropanol (compare Figure 2, spectra a and e). The absolute amplitude of the ENDOR doublet from the sample obtained with [5′,5′-$^2H_2$]-AdoCbl is however smaller than that of the doublet obtained with deuterated substrate. The drop in amplitude may be due, in part, to a 1/3 probability of finding ^1H instead of ^2H at the closest position of the methyl group of 5′-deoxyadenosine when [5′,5′-$^2H_2$]-AdoCbl and unlabeled substrate are used. There could also be a partial washout of deuterium during multiple enzymatic turnovers with unlabeled substrate, although the deuterium isotope effect would discriminate against such washout. However, the identical ^2H ENDOR frequencies in the two spectra indicate that ^2H which enters the system via C1 of *S*-2-aminopropanol or via C5′ of deoxyadenosine ends up in the same position with respect to the organic radical intermediate. Given the possibility of exchange of hydrogen atoms in these radical reactions, the ^2H ENDOR results by themselves do not require that the ^2H giving rise to the ENDOR signal resides on 5′-deoxyadenosine.

^{13}C ENDOR. The Mims ENDOR spectrum obtained from the lower field maximum of the absorption spectrum of the radical (Figure 1b) for the sample prepared with [U-^{13}C-ribosyl]-AdoCbl and unlabeled *S*-2-aminopropanol is presented in Figure 3Aa. The corresponding spectrum from a sample prepared with unlabled cofactor and unlabeled substrate (Figure 3Ab) contains all of the same features except for the well-defined set of resonances that is centered about the ^{13}C Larmor frequency in Figure 3Aa. The difference spectrum (Figure 3Ac) highlights the ^{13}C transitions. The most prominent peaks occur at the outer edges of the pattern and correspond to a splitting of 1.0 MHz ($A_\perp$). These transitions are assigned to the orientations of the magnetic field that are perpendicular to the unique axis of an axially symmetric ^{13}C hyperfine coupling tensor. A weaker peak occurs 0.25 MHz below the Larmor frequency. The corresponding ^{13}C transition from the opposite electronic submanifold is not resolved at this magnetic field setting. However, the observed, lower frequency peak implies a hyperfine coupling of about 0.5 MHz. This weaker coupling is assigned to $A_{||}$. In using relative peak amplitudes to assign nuclear spin transitions in Mims ENDOR, one must consider the weighting of the ENDOR response according to the selected value of τ, the delay between the first two microwave pulses. For the ^{13}C coupling, at any orientation, the product, $A\tau < 0.3$ (where A is the nuclear hyperfine coupling constant), is safely within the regime where the ENDOR spectrum is not significantly affected by Mims blind spots *(19)*.

The assignments given above lead to the following ^{13}C superhyperfine coupling[3] parameters: $A_{||} = +0.5$ MHz, and $A_\perp = \pm 1.0$ MHz (relative signs only). If like signs are chosen (i.e., if the coupling does not pass through zero at any orientation), one obtains an isotropic component $A_0 = +0.83$ MHz and (using the point−dipole approximation) a distance, r, of 4.9 Å between the center of unpaired spin on the radical and the ^{13}C nucleus. If the opposite sign

[2] A "typical" α-deuteron hyperfine coupling tensor of ∼(13, 4.2, 8.7) MHz is expected for the ^2H remaining on C1 of the radical.

[3] The terminology, superhyperfine coupling, is used to signify coupling between an unpaired electron spin on one molecule and a nuclear spin on another molecule.

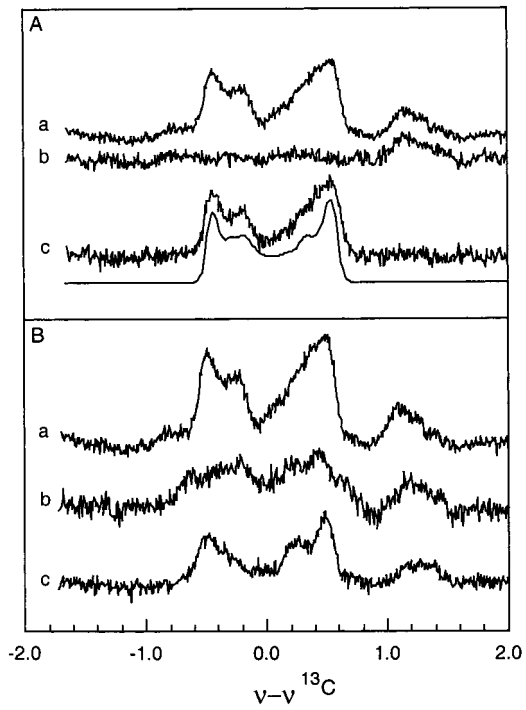

FIGURE 3: Mims ENDOR spectra with [U-^{13}C ribosyl]-AdoCbl (A) and the magnetic field dependence (B) of the ^{13}C Mims ENDOR. Panel A shows Mims ENDOR spectra from the substrate radical in EAL, generated with unlabeled substrate: (Aa) [U-^{13}C ribosyl]-AdoCbl; (Ab) unlabeled cofactor. The difference spectrum, Aa − Ab, is shown in Ac. The smooth curve below (Ac) is a simulation of the difference spectrum. Experimental conditions for Aa and Ab: $B_0 = 340.5$ mT; $\tau = 0.410$ μs; $t_{rf} = 8$ μs; $\nu_e = 9.697$ GHz. Each point is sum of 6400 echoes; pulse sequence repetition rate = 1.0 kHz; $T = 18$ K. For the simulation, a g value of 1.993 for observation was used. The assumed principal values of the ^{13}C hyperfine coupling tensor were (−1.05, −1.05, +0.6) MHz; and those of the g-tensor were (1.990, 1.990, 2.000). Panel B shows the magnetic field dependence of ^{13}C Mims ENDOR for the same sample used in obtaining trace 3Aa. Traces 3Ba−c were obtained at magnetic fields of 340.5, 346.5, and 352.0 mT, respectively. Other experimental conditions were the same as for Aa.

combination holds, then $A_0 = -0.5$ MHz and $r = 3.4$ Å. The latter combination leads to the more satisfying physical result—namely, that a substantial isotropic superhyperfine coupling is associated with a short distance. The former sign combination gives a larger isotropic coupling at a much longer distance. A negative sign for A_0 is also expected from a spin polarization model in which the half-occupied p orbital of the radical has a small overlap with the "hydrogen end" of a C5′-H σ orbital (*20*). Thus, the ^{13}C ENDOR spectra are most compatible with a distance[4] between C5′ of the cofactor and C1 of the substrate of 3.4 ± 0.2 Å.

A calculated ENDOR spectrum is shown immediately below trace 3Ac. An axially symmetric g-tensor having weak anisotropy was assumed for the radical as a rough approximation to the orientation selection arising from the dipole−dipole coupling between the radical and the Co^{2+}. No attempt was made to account for the complex orientation selection created by the unresolved nuclear hyperfine splittings within the envelope of the radical doublet. The principal axes of the g-tensor and the ^{13}C superhyperfine tensor were assumed to be collinear. Though approximate, this approach reproduces the general shape of the ^{13}C ENDOR spectra using parameters very similar to those obtained directly from the spectra.

The magnetic field dependence of the ^{13}C ENDOR was examined (Figure 3B). Spectra obtained at 340.5 and 352.0 mT, near each of the two local maxima, produce very similar ^{13}C ENDOR spectra (Figure 3Ba,c). The major difference between them is that in the spectrum obtained at the lower field, the ENDOR transition at about −0.25 MHz is resolved and the transition near +0.25 MHz is a shoulder. At 352.0 mT, however, the opposite is true. The fact that the magnetic field-dependent amplitudes of the ^{13}C ENDOR spectra track the amplitude of the radical doublet provides further assurance that the ENDOR response is associated with the substrate radical.

DISCUSSION

The low- and high-field maxima in the CW EPR doublet signal of the radical correspond to a common set of magnetic field orientations, namely, those perpendicular to the z-axis of the reference frame of Co^{2+} (V. Bandarian and G. H. Reed, manuscript in preparation). Thus, the perpendicular field direction is correlated with the sharp "perpendicular" features at the extremes of the ^{13}C ENDOR pattern. The middle region of the EPR absorption of the radical, which is richer in contributions from the parallel orientation of the magnetic field in the Co^{2+} axis system, yields ENDOR spectra having stronger parallel features. These observations indicate that the unique axis of the ^{13}C superhyperfine coupling tensor is approximately parallel to the z-axis of Co^{2+}. Analysis of the Co^{2+} radical spin−spin interactions indicates that C1 of the substrate radical lies approximately along the z-axis of Co^{2+} and that the unique axis of the half-occupied p orbital is approximately parallel to the z-axis in the Co^{2+} reference frame (*21*). The CW EPR and the pulsed ENDOR data indicate that the unique axis of the ^{13}C superhyperfine coupling tensor is approximately coincident with the z-axis of Co^{2+}.

The ∼3.4 Å distance between C5′ and the unpaired electron constrains the range of allowable distances between C1 and the nearest ^{2}H on the C5′ methyl group. The C5′-methyl group acquires three deuterium atoms after a few turnovers with the labeled substrate (*8*) before freeze-quenching. Given the C1−C5′ distance, modeling shows that there must be at least one ^{2}H from the 5′-trideuteriomethyl group within ∼3.3 Å of C1. This long a distance could only apply if all three deuterium atoms were arranged strictly symmetrically about (and thus equidistant from) the half-occupied p orbital of C1. In the far more likely case that the three couplings are not equivalent, the absence of multiple ^{2}H doublets in the ENDOR spectra of Figure 2 would indicate that one deuterium is much closer to C1 than are the other two. This situation can occur, for example, if the ^{2}H−C5′ bond lies close to the C5′−C1 interspin vector. The distance between C1 and the ^{2}H could become as small as 2.3 Å.

The present results lead to a schematic model of the radical and 5′-deoxyadenosine as shown in Figure 4. The model explains the observation of substantial superhyperfine cou-

[4] The implicit assumption is that the C5′-methyl of the ribosyl moiety is closest of the five labeled carbons. The rapid falloff of ENDOR intensity with hyperfine coupling (interspin distance) suggests that only the closest ^{13}C will give rise to an ENDOR signal.

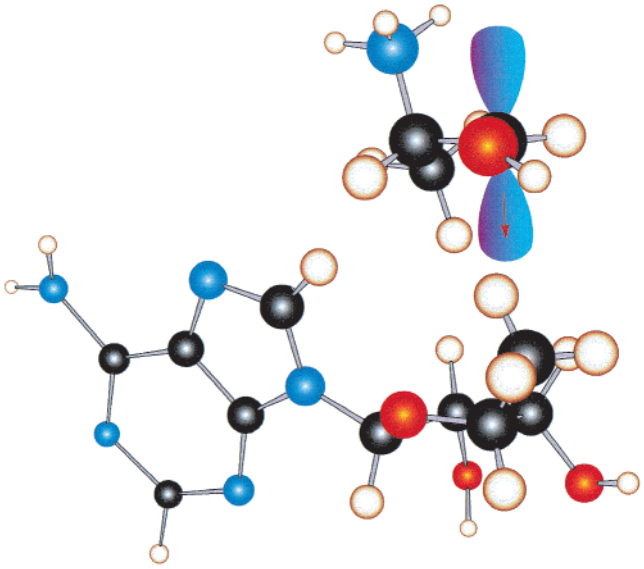

FIGURE 4: Ball and stick representation of the interaction of the radical of *S*-2-aminopropanol and 5′-deoxyadenosine in the active site of EAL. The distance between C1 of the radical and C5′ of deoxyadenosine (3.4 Å) is obtained from the ^{13}C ENDOR data. Other intermolecular distances and relative orientations are arbitrary.

plings between the unpaired electron and both ^{2}H and ^{13}C. The scalar (or contact) component of the ^{13}C coupling indicates that a small amount unpaired spin is transferred, intermolecularly, from the substrate radical to the C5′ carbon. This transfer likely occurs via spin polarization from overlap of a C5′-H σ orbital with the half-occupied p orbital of the radical. The finding of C5′ in contact with the substrate radical is consistent with a mechanism in which a 5′-deoxyadenosyl radical, formed after substrate binding, approaches the substrate and abstracts a hydrogen atom directly from C1. Proximity of the C5′ methyl group to the substrate radical also allows for direct regeneration of the 5′-deoxyadenosyl radical through loss of a hydrogen atom to the product radical at C2 following rearrangement. Thus, C5′ of the 5′-deoxyadenosyl radical must shuttle a distance of ~7 Å between its resting site in the carbon−cobalt bond of the uncleaved coenzyme and a position adjacent to C1 and C2 of the substrate/product. Rotation of the ribosyl moiety about the glycosidic bond provides a possible mechanism for the shuttle movement. Such a rotation has recently been suggested for C5′-radical to substrate accessibility in diol-dehydratase (*22*).

Saturating concentrations of *S*-2-aminopropanol were used in making up the samples for these ENDOR experiments. Hence, the experiments show that the C5′-methyl of 5′-deoxyadenosine is in a position to mediate the hydrogen transfers under V_{max} conditions. These structural results support the notion that the large ^{3}H KIE on washout of ^{3}H from labeled cofactor arises from hydrogen atom tunneling in the abstraction steps of EAL.

REFERENCES

1. Abeles, R. H., and Dolphin, D. H. (1976) *Acc. Chem. Res. 9*, 114−120.
2. Babior, B. M. (1982) in *B_{12}* (Dolphin, D., Ed.) John Wiley & Sons, Inc., New York.
3. Weisblat, D. A., and Babior, B. M. (1971) *J. Biol. Chem. 246*, 6064−6071.
4. Boas, J. F., Hicks, P. R., Pilbrow, J. R., and Smith, T. S. (1978) *J. Chem. Soc., Faraday Trans. 2 74*, 417−430.
5. Cleland, W. W. (1982) *Crit. Rev. Biochem. 13*, 385−428.
6. O'Brien, R. J., Fox, J. A., Kopczynski, M. G., and Babior, B. M. (1985) *J. Biol. Chem. 260*, 16131−16136.
7. Bandarian, V., Poyner, R. R., and Reed, G. H. (1999) *Biochemistry 38*, 12403−12407.
8. Bandarian, V., and Reed, G. H. (2000) *Biochemistry 39*, 6250−6257.
9. Harkins, T. T., and Grissom, C. B. (1994) *Science 263*, 958−960.
10. Bandarian, V., and Reed, G. H. (1999) *Biochemistry 38*, 12394−12402.
11. Hamilton, J. A., Tamao, Y., Blakley, R. L., and Coffman, R. E. (1972) *Biochemistry 11*, 4696−4705.
12. Parkin, D. W., Leung, H. B., and Schramm, V. L. (1984) *J. Biol. Chem. 259*, 9411−9417.
13. Parkin, D. W., and Schramm, V. L. (1987) *Biochemistry 26*, 913−920.
14. Rising, K. A., and Schramm, V. L. (1994) *J. Am. Chem. Soc. 116*, 6531−6536.
15. Suh, S. J., and Escalante-Semerena, J. C. (1995) *Bacteriology 177*, 921−925.
16. Zehnder, A. J. B., and Wuhrmann, K. (1976) *Science 194*, 1165−1166.
17. Mims, W. B. (1965) *Proc. R. Soc. A* (*London*) *283*, 452−457.
18. Scholes, C. P. (1979) in *Multiple Electron Resonance Spectroscopy* (Dorio, M. M., and Freed, J. H., Eds.) pp 297−330, Plenum, New York.
19. Hoffman, B. M., DeRose, V. J., Doan, P. E., Gurbiel, R. J., Houseman, A. L. P., and Tesler, J. (1993) *Biol. Magn. Reson. 13*, 151−218.
20. Wertz, J. E., and Bolton, J. R. (1986) *Electron Spin Resonance*, Chapman and Hall, New York.
21. Bandarian, V. (1998) Ph.D. Thesis, University of Wisconsin, Madison.
22. Masuda, J., Shibata, N., Morimoto, Y., Toraya, T., and Yasuoka, N. (2000) *Structure Fold Des. 8*, 775−788.

BI001865S